Journal of Nuclear Materials 463 (2015) 634–639

Contents lists available at ScienceDirect

Journal of Nuclear Materials

journal homepage: www.elsevier.com/locate/jnucmat

Impact of localized gas injection on ICRF coupling and SOL parameters in JET-ILW H-mode plasmas

E. Lerche [b,c,*,1], M. Goniche [d], P. Jacquet [c], D. Van Eester [b], V. Bobkov [e], L. Colas [c], A. Czarnecka [f], S. Brezinsek [g], M. Brix [c], K. Crombe [b], M. Graham [c], M. Groth [h], I. Monakhov [c], T. Mathurin [i], G. Matthews [c], L. Meneses [j], C. Noble [c], V. Petrzilka [k], F. Rimini [c], A. Shaw [c], JET-EFDA Contributors [a,2]

[a] JET-EFDA, Culham Science Centre, Abingdon OX14 3DB, UK
[b] LPP-ERM-KMS, TEC Partner, 1000 Brussels, Belgium
[c] CCFE, Culham Science Centre, Abingdon OX14 3DB, UK
[d] CEA, IRFM, F-13108 Saint-Paul-Lez-Durance, France
[e] Max-Planck-Institut für Plasmaphysik, Garching, Germany
[f] IPPLM, 01-497 Warsaw, Poland
[g] Forschungszentrum Jülich, Institute of Energy Research, Jülich, Germany
[h] Aalto University, 02015 Espoo, Finland
[i] École des Mines de Paris, 75006 Paris, France
[j] Instituto de Plasma e Fusão Nuclear, Instituto Superior Técnico, Lisbon, Portugal
[k] Institute of Plasma Physics, Prague, Czech Republic

ARTICLE INFO

Article history:
Available online 13 November 2014

ABSTRACT

Recent JET-ILW [1,2] experiments reiterated the importance of tuning the plasma fuelling in order to optimize ion cyclotron resonance frequency (ICRF) heating in high power H-mode discharges. By fuelling the plasma from gas injection modules (GIMs) located in the mid-plane and on the top of the machine instead of adopting the more standardly used divertor GIMs, a considerable increase of the ICRF antenna coupling resistances was achieved with moderate gas injection rates ($<1.5 \times 10^{22}$ e/s). This effect is explained by an increase of the scrape-off-layer density in front of the antennas when mid-plane and top fuelling is used. By distributing the gas injection to optimize the coupling of all ICRF antenna arrays simultaneously, a substantial increase in the ICRF power capability and reliability was attained. Although similar core/pedestal plasma properties were observed for the different injection cases, the experiments indicate that the RF-induced impurity sources are reduced when switching from divertor to main chamber gas injection.

1. Introduction

Although ion cyclotron resonance heating (ICRH) is an auxiliary heating technique based on the absorption of radio-frequency (RF) waves by the various species in the bulk plasma, the edge/scrape-off layer (SOL) properties have a decisive influence on its overall performance: (i) the fast waves launched by the antennas are evanescent at low densities ($\sim 10^{18}/m^3$) and the actual density profile in the SOL will impose the maximum power attainable for a given voltage V_{ant} applied to the antennae, $P_{icrf} \propto R_{ant} \times (V_{ant})^2$, as characterized by the coupling resistance R_{ant}; (ii) the RF fields produced in the SOL are typically large and strongly inhomogeneous, leading to ponderomotive forces and particle drifts that can locally modify the SOL properties [3,4]; (iii) due to the different ion and electron velocities along the magnetic field lines and the low SOL collisionality, the parallel RF electric fields induce rectified potentials (plasma biasing) that can accelerate ions in the SOL to energies up to a few hundreds of eV inducing heat loads to plasma-facing components (PFCs) and sputtering of plasma-facing material during ICRF operation [5–8]; (iv) part of the launched wave spectrum does not penetrate into the plasma (coaxial modes, surface waves, etc.) and thus may be absorbed at the plasma periphery and impact on the local pedestal/SOL characteristics. In practice, the optimization of ICRF heating in large tokamaks consists in finding the best compromise to simultaneously enhance the antenna coupling while minimizing edge power absorption and

* Corresponding author at: Royal Military Academy, Physics Department, Av. de la Renaissance 30, B1000, Brussels, Belgium.
E-mail address: elerche@jet.efda.org (E. Lerche).
[1] Presenting author.
[2] See the Appendix of F. Romanelli et al., Proceedings of the 24th IAEA Fusion Energy Conference, 2012, San Diego, USA.

http://dx.doi.org/10.1016/j.jnucmat.2014.10.074
0022-3115/

mitigating RF sheath rectification effects, in particular in full-metal machines such as AUG, JET-ILW and ITER.

After installation of a full-metal ITER-like wall (ILW) in JET, with most of the main chamber PFCs made from beryllium (Be) and a tungsten (W) divertor [1,2], accumulation of heavy impurities (in particular W) has become a concern in high power H-modes with low fuelling rates since, aside from degrading the plasma performance, it can lead to radiative collapse of the discharges. ASDEX Upgrade [9] and more recently JET-ILW [10] experiments have shown that an efficient way of avoiding this deleterious central impurity accumulation is to provide a localized heat source to the plasma core, either by electron cyclotron (ECRH) or by ion cyclotron resonance heating (ICRH) as the resulting peaked temperature profiles near the plasma centre have a direct impact on the transport of the high-Z impurities and can expel them from the core [11,12]. While AUG is equipped with both ECRH and ICRH, only the latter is available in JET.

Presently, JET is equipped with 4 ICRF antenna arrays composed of 4 straps each (see Fig. 1). To cope with the power reflections due to impedance mismatch that occurs due to fast plasma changes such as during ELMs, antennas A and B are connected to a common RF generator via 3 dB hybrid couplers while antennas C and D are connected together in the so called conjugate-T configuration [13]. The total power capability of the ICRF system in JET in this configuration is estimated to be about 9–10 MW, considering ~6 MW of generator power feeding each pair of antennas and typical Ohmic losses in the transmission lines and antenna structures. However, because of the unfavorable coupling conditions often observed in high power H-modes (low SOL density, steep edge gradients, etc.), the power coupled to H-mode discharges is considerably lower, since the maximum allowed voltage on the antenna straps (30–35 kV) is reached before the generators get to their full power capability. Therefore, increasing the antenna coupling thus decreasing the antenna voltages for given input power is essential to enhancing the performance of the ICRF system.

To optimize the ICRH power that can be launched into high power H-mode discharges in JET in view of impurity control, dedicated experiments have been performed in order to (i) maximize the coupled power (coupling resistance) by tailoring the SOL density profiles via localized gas injection close to the antennas, (ii) minimize the RF-induced impurity sources caused by RF sheath rectification effects and (iii) fine-tune the RF heating scenario (resonance position, minority concentration, etc.) to optimize the core plasma heating. The first two points will be addressed in this paper while the scenario optimization as well as the efficiency of ICRF heating on the mitigation of core impurity accumulation in high performance JET discharges are described elsewhere [10,14]. The use of local gas puffing to enhance the RF coupling resistance of ICRF antennae located close to the gas injection inlets was inspired on the results obtained in AUG [15,16] and in JET-C [17], but not developed for high performance plasma operation in JET-ILW. This study is part of a broader inter-machine effort that focuses on optimizing ICRH for ITER and future fusion devices [18].

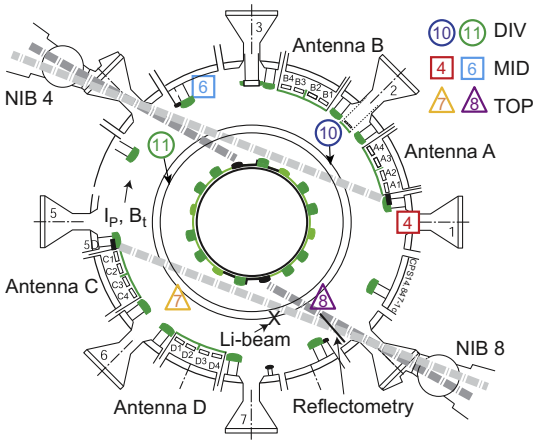

Fig. 1. Top view of JET illustrating the toroidal positions of the 4 ICRF antenna arrays and the location of several gas injection modules: GIMs 10/11 (outer and inner divertor rings), GIMs 4/6 (mid-plane valves) and GIMs 7/8 (top valves). The SOL density diagnostics (Li-beam and reflectometry) are also indicated.

To systematically study the influence of the location of the gas injection on the RF coupling resistances of the various antennas and on the SOL parameters in JET-ILW, a series of similar low triangularity H-mode discharges with $B_0 = 2.7$ T, $I_P = 2.5$MA, $P_{NBI} = 13$–15 MW and $n_0 = 7$–$8 \times 10^{19}/m^3$ were performed with deuterium fuelling from different toroidal and poloidal locations in the torus. The mid-plane antenna-separatrix distance was kept fixed at ~10 cm in all discharges. The location of the gas injection modules (GIMs) used and the ICRF antennae positions are shown in Fig. 1: Divertor injection modules consisting of 48 toroidally distributed inlets (circles: GIM 10 and 11), mid-plane injection modules which are single inlets or a small poloidal row (squares: GIM 4 and 6), top single injection modules (triangles: GIM 7 and 8). Central hydrogen minority ICRH at $f = 42$ MHz (dipole phasing) with $P_{icrf} = 3$ MW and $n_H/n_e \sim 5\%$ was adopted and three deuterium levels were used in each discharge to also study the influence of the gas rate on the coupling resistances of the antennas.

2. Effect of localized gas-injection on RF coupling resistance

In view of optimizing the antenna-plasma coupling, a series of similar discharges using gas fuelling from different GIMs with different injection rates was performed and the coupling resistances of the various antennas were monitored. The results are summarized in Fig. 2, where the coupling resistances (averaged over 4 straps) of antennas A, B and C/D are plotted as function of the total deuterium injection rate. Antennas C and D are assumed to have the same coupling resistance since they are connected in conjugate-T configuration and RF measurements of each individual T-branch are not available. The data correspond to 1s time averages of the inter-ELM ICRF coupling signals during intervals with constant gas rate. Strike point sweeps of 4 Hz were used to control the divertor heat loads and the ELM frequency varied between 15 and 45 Hz, depending on the gas injection adopted. The plasma core and pedestal parameters as well as the confinement properties were similar in the studied discharges and only a small increase of the plasma density with gas rate was observed for all injection cases (<20% in the 0.5–2 $\times 10^{22}$ e/s range).

The results shown in Fig. 2 demonstrate the beneficial effect of adopting localized gas injection as opposed to quasi-homogenous divertor injection on the RF coupling resistances of the ICRF antennas: antenna A is mostly sensitive to the closest gas injection (GIM4), antenna B to GIM6, and the compound antenna C/D to GIMs 7 and 8 (see Fig. 1). Distributed divertor fuelling (GIMs 10 and 11) leads to near-SOL fuelling and therefore to the poorest coupling in all antennas (located in the far-SOL), independently of the gas level applied. From the mid-plane fuelling results (GIM4 and 6), one sees that the closest the gas injection point the more efficient is the enhancement of the coupling resistance, especially at higher injection rates. The results of the top-injection cases (GIM7 and 8) are less straightforward to interpret, since despite their different relative distances to antenna C + D they have comparable impact on their coupling resistances. Moreover, these GIMs also have a considerable influence on antennas A and B, pointing to the fact that not only injection proximity but also magnetic connection via flux tubes plays a role in the far-SOL density tailoring process.

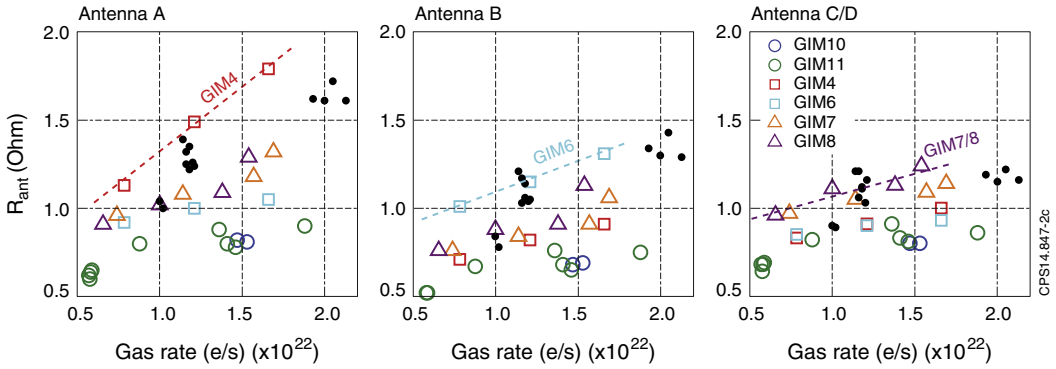

Fig. 2. Coupling resistances of the various ICRF antennas as function of the total D_2 injection rate for different fuelling locations: Divertor injection (circles: GIMs 10 and 11), mid-plane injection (squares: GIMs 4 and 6), top injection (triangles: GIMs 7 and 8). The data correspond to 1s averages of the inter-ELM RF signals at constant gas rate. The black dots represent the results with the best gas injection mix found to simultaneously improve the coupling of all antennas (GIMs 4 + 6 + 8).

Since the overall ICRF performance has to be optimized, the coupling resistances of all antennas need to be simultaneously improved, keeping in mind that the gas injection levels have to be kept as low as possible to not impact the plasma confinement. Based on the results from the individual GIMs, an optimized gas injection scheme consisting of a combination of main chamber fuelling (30% from GIM 4, 30% from GIM 6 and 40% from GIM 8) was found to be best suited to accomplish this task. The results are represented as black dots in Fig. 2. With this distributed gas injection scheme a homogeneous tailoring of the far-SOL density is achieved and all antennas operate above $R_{ant} = 1\ \Omega$ with moderate deuterium injection rate ($\geqslant 1.2 \times 10^{22}$ e/s). In these conditions the ICRF system was capable of regularly supplying ~6 MW of coupled power in ELMy H-mode plasmas.

To further investigate the effect of local gas injection on the RF coupling properties, simulations using a fast wave only 1D slab coupling code were performed. As dedicated SOL density measurements close to the ICRF antennas are not available in JET, the inter-ELM density profiles reconstructed from reflectometry measurements [19] taken toroidally away from the antennae were used as input to the coupling code to estimate the coupling resistance an antenna would have if located close to the diagnostics, i.e. in between antennas A and D (see Fig. 1). The results of the simulations are shown in Fig. 3-middle together with an example of the density profiles measured with divertor (GIM11), mid-plane (GIM4) and top (GIM7) gas fuelling at similar injection rates (Fig. 3-left). The dependence of the calculated coupling resistances on the antenna – cut-off distance (width of the evanescence region) is depicted in Fig. 3-right. The calculations are normalized to give the experimental coupling resistance measured in antenna A with GIM11 fuelling at maximum gas rate ($R_{ant} = 0.9\ \Omega$).

Since the measured densities do not correspond to the actual densities in front of the ICRF antennas, RF modeling can at best provide qualitative insight whereas the actual localized SOL perturbations close to the gas injection points are probably stronger. The simulations indeed capture the general aspects of the impact of local gas injection on the RF coupling resistances: mid-plane and top gas injection (in particular using GIM4 and GIM7 which are magnetically connected to the density measurements) show higher coupling resistances than when divertor fuelling is adopted. Moreover, similar to what was observed in the experiments, when main chamber fuelling is used the coupling resistances increase linearly with the gas injection rate while with divertor fuelling the values are only weakly sensitive of the amount of gas used. Although GIM8 is located right on top of the density diagnostics and has a clear impact on the measured coupling resistances of all ICRF antennas, its influence on the measured SOL densities is limited as seen by the lower coupling resistance values obtained in the modeling. Once more, this points to the fact that on top of proximity, magnetic connection between the antennas and the gas injection region also influences the far-SOL density pattern, as will be discussed later. It is interesting to note how sensitive the calculated coupling resistances are to the far-SOL density profiles, as seen from the relatively mild differences between the profiles shown in Fig. 3-left for the different injection cases and corroborated by EDGE2D simulations, which nevertheless translate into a considerable increase of the calculated coupling resistances. This sensitivity is confirmed on Fig. 3-right, which shows that a

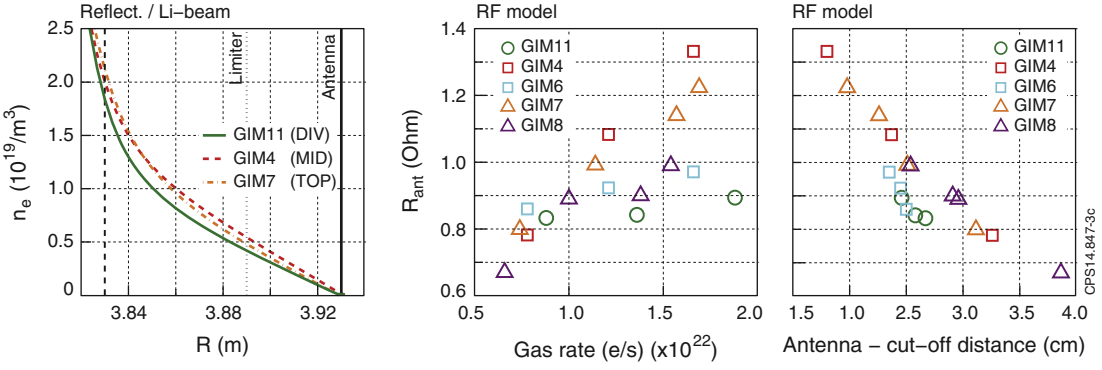

Fig. 3. (left) Density profiles reconstructed from reflectometry measurements for 3 gas injection cases: divertor (solid: GIM11, 1.85e22 e/s), mid-plane (dashed: GIM4, 1.65e22 e/s) and top (dash-dotted: GIM7, 1.6e22 e/s); (middle) coupling resistances calculated by a 1D slab RF coupling code using the experimental density profiles from reflectometry for the various gas injection cases; (right) coupling resistances as function of the fast wave evanescence width for $f = 42$ MHz and dipole phasing.

shift of less than 1 cm in the fast wave density cut-off position can lead to this order of coupling variations.

3. Local perturbation of far-SOL density

The large variations of the RF coupling resistances observed with localized gas injection suggest that the electron density profiles in front of the various antennas for a given fuelling configuration are not the same, contrary to the simple intuition based on toroidal axisymmetry. The localized modification of the SOL density profiles is possible because the antennas are in-fact retracted by a few cm from the various toroidally distributed outer poloidal limiters and de facto a secondary SOL or even a private region (with reduced parallel connection length) develops in between two adjacent poloidal limiters. To investigate this effect in more detail, the individual coupling resistances of the antenna straps were analyzed as function of the distance to the gas injection point. In Fig. 4-left the relative variations of the strap coupling resistances $\Delta R/R_{ref}$ of antennas A and B for 4 similar discharges with mid-plane and top gas injection are represented as function of the toroidal GIM-strap distance. The coupling resistances measured in a divertor gas fuelling pulse (GIM11) with similar injection rate were used as reference (R_{ref}) to estimate the relative coupling variations for each strap.

The local nature of the gas injection influence on the RF coupling is evident in the mid-plane fuelling cases (GIMs 4 and 6): The coupling enhancement decreases exponentially with the GIM-strap distance with a toroidal decay length of $\lambda_z \approx 2$ m ($\phi \approx 0.5$ rad), in good agreement with similar studies performed in AUG, where a toroidal decay of $\phi \approx 0.6$ rad was found [16]. In contrast, with top gas injection (GIMs 7 and 8) all straps are affected in a similar way (as also for antenna C/D, not shown) suggesting a global (toroidally symmetric) enhancement of the far-SOL density. The exponential decay of $\Delta R/R_{ref}$ in the toroidal direction (z) seen for the mid-plane fuelling cases indicates that an essentially uniform effect is responsible for the local electron density perturbation, making the SOL density decay at a rate proportional to the density value itself, $dN_e/dz = -N_e/\lambda_z$. This suggests that the diffusion of the injected neutrals – which is uniform in the poloidal and toroidal directions – is the dominant player in the local SOL density build-up around the injection point, including the region behind the outer poloidal limiter, where the large RF electric fields may contribute to the neutral ionization. For the top injection cases, the toroidal homogeneity of the coupling variations indicates that the ionization of the neutrals in flux tubes connected to the ICRF antennas (predominantly outside the poloidal limiter shadow) is now the main mechanism for the density enhancement in the far SOL since the ionization process in the SOL is, to first order, toroidally symmetric. On the other hand, it strongly depends on the radial SOL profiles locally 'seen' by the injected neutrals and geometrical effects such as the radial distance between a specific injection valve and the last closed magnetic surface as well as the magnetic topology near the injection point can also influence the results. Although top gas injection has the potential of improving the coupling of all antennas at the same time, a higher fuelling rate would be needed for reaching the coupling improvements attained with localized (mid-plane) gas injection. The symmetry between the mid-plane results, GIM4 (counter-current) and GIM6 (co-current), suggest that drift/plasma flow effects are not major players in the density build-up in the far-SOL in these conditions. It has to be mentioned that similar studies using different divertor configurations (lower pumping) show hints of a privileged density enhancement in the counter-current direction.

The sensitivity of the coupling resistances to the far-SOL electron density can be used to estimate the density profiles in front of each antenna strap if neglecting parallel transport effects. This was made by using the simple 1D RF coupling model described earlier to determine the best density profile needed for matching the measured coupling resistance enhancements as function of the GIM-strap distance shown in Fig. 4-left. The calculations were normalized to match the experimental coupling resistance of antenna A during the discharge with divertor (GIM11) fuelling, $R_{ref} = 0.9\ \Omega$. The coupling enhancement ($\Delta R/R \sim 50\%$) obtained with the RF code using the density profiles measured by reflectometry with GIM4 fuelling (~3 m away) is shown in Fig. 4-left to illustrate the good agreement between the modeling and the experiments when the SOL electron density is modified. Because the simulations are only constrained to a 0D quantity (namely the coupling resistance), different density profiles can, a priori, be used in the calculations to match the experimental results. To keep the simulations as realistic as possible, an analytical density profile parameterized to best fit the reflectometry/Li-beam data was used, with an exponential decay in the region between the plasma separatrix

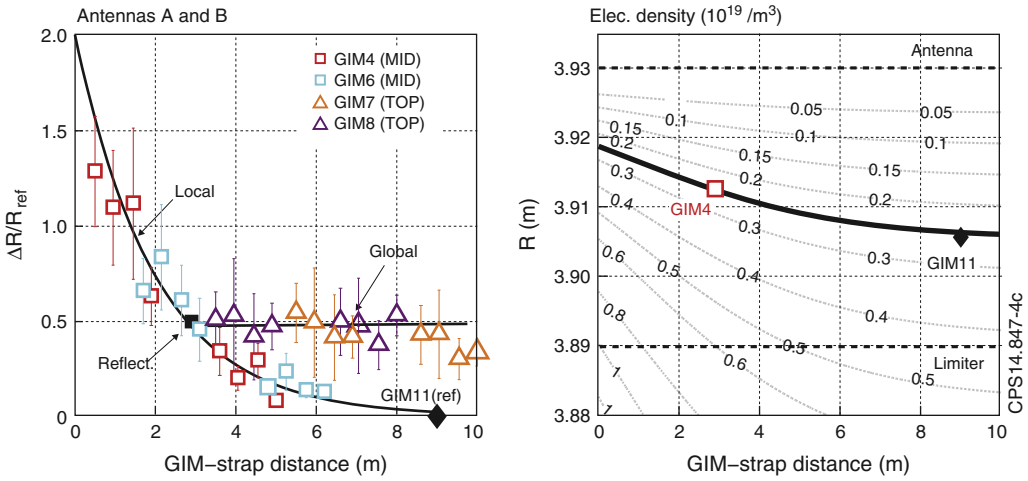

Fig. 4. (left) Relative coupling resistance increase of the individual antenna straps with respect to a divertor fuelled discharge (GIM11, 1.85e22 e/s) for two mid-plane (GIM4 and GIM6, 1.65e22 e/s) and two top gas injection pulses (GIM7 and GIM8, 1.6e22 e/s) as function of the toroidal GIM-strap distance; (right) 2D density profile reconstructed from RF coupling modeling by finding the density profiles (parameterized to the reflectometry data) that best fit the experimental coupling measurements in each toroidal position for mid-plane gas injection. The thick solid curve represents the cut-off density for the mid-plane gas injection case while the dotted line indicates the cut-off position if divertor fuelling would be used (assuming toroidally homogeneous far-SOL density).

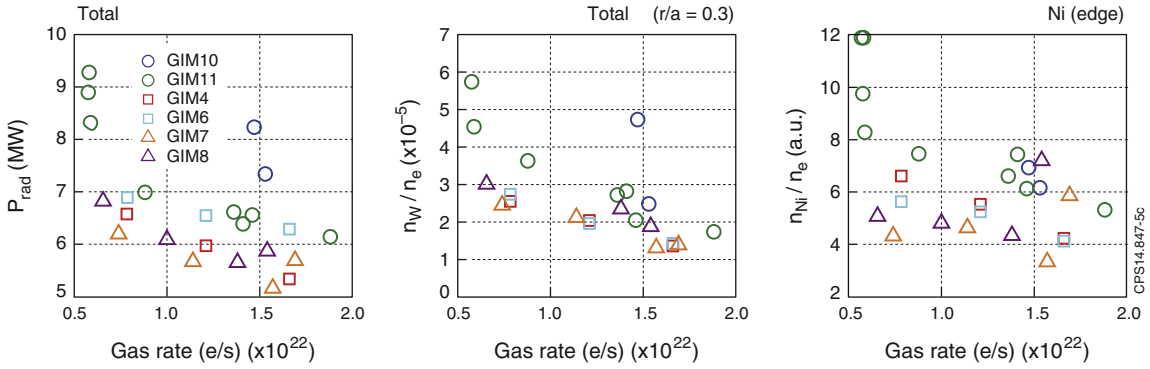

Fig. 5. (left) Total radiation, (middle) W concentration at mid-radius and (right) edge Ni concentration (in a.u.) as function of the gas rate for the various fuelling cases studied.

(R = 3.83 m) and the poloidal limiter (R = 3.88 m) followed by a linear decrease with radius from the limiter to the antenna position (R = 3.93 m). The resulting 2D density profile in the shadow of the limiter obtained with this procedure representing 1.65×10^{22} e/s of deuterium being injected in the mid-plane is illustrated in Fig. 4-right. The density values given in the contour lines are in $10^{19}/m^3$. The cut-off density of the fast wave for the main toroidal mode excited by the antenna in dipole phasing configuration is represented as the thick solid line whilst the cut-off for the reference GIM11 pulse assuming toroidally homogeneous density is shown as a dashed line. The cut-off positions obtained directly from reflectometry measurements in the discharges with GIM11 (diamond) and GIM4 (square) fuelling are also represented, indicating that the density parameterization adopted is in good agreement with the measured profiles. The results show that when local mid-plane gas puffing is used, the antenna – cut-off distance is reduced by ~1.4 cm for toroidal distances lower than $\lambda_z \approx 2$ m (e.g. antenna A with GIM4 injection) and by ~0.7 cm for intermediate distances (e.g. antenna B with GIM6 injection) with respect to divertor injection. Based on the RF coupling simulations using the reflectometry profiles (Fig. 3-right), such shifts would lead to coupling resistance increases of respectively 0.9 Ω and 0.7 Ω, in good agreement with the measured values shown in Fig. 2.

4. Effect of local gas injection on RF-induced impurities

Previous L-mode studies have shown that the main heavy impurities induced by RF sheath rectification effects in JET-ILW are Ni and W [7], which are sputtered from structures located in the main vacuum chamber (Ni from Inconel and recessed areas close to the antennas and W from e.g. the NBI shine-through plates) and in the W-coated divertor aprons rather than in the bulk divertor [20]. In fact, the here reported experiments indicate that distributed main chamber fuelling is favorable for reducing the RF-induced impurities during ICRF assisted H-mode discharges. This is illustrated in Fig. 5, where the total radiated power (left) together with the W (middle) and Ni (right) concentrations are represented as function of the gas injection rate for different fuelling locations (same pulses and time intervals as considered previously). The radiation data were normalized to the line integrated densities and multiplied by the average density value of all points to allow a quantitative comparison with the total auxiliary power applied (P_{nbi} = 14 ± 1 MW with constant P_{icrf} = 3 MW). The W concentration is inferred from line emission of highly ionized W ions and corresponds to the concentration around r/a = 0.3 m [21] while the Ni content is estimated from edge spectroscopy in the confined region [22].

Two features are clearly visible in the results: (i) the radiation as well as the impurity levels decrease with increased gas fuelling in all cases, as the SOL is locally cooled and the sputtering yield of the ions is reduced, as commonly observed in JET-ILW and W-divertor machines [2,20]. A minimum gas injection level is required to impact on the energy of the impinging ions as seen by the strong increase of all quantities below $\sim 6 \times 10^{21}$ e/s; (ii) the total radiation is about 15–20% lower in the discharges where main gas chamber fuelling is used (except for GIM6) as opposed to divertor fuelling, in agreement with the lower levels of W and Ni observed in these cases. This indicates that the RF-induced impurity sources are partly mitigated when main chamber fuelling is used. A similar effect was observed in AUG when deuterium injection localized close to the RF antennas was used [15,16].

The exact mechanisms that cause the reduction of RF induced plasma-wall interaction when main chamber gas injection is used are still to be identified and required complex modeling of the antenna fields in realistic geometry, RF sheath rectification effects and their impact on the SOL particle acceleration and on the wall material sputtering, which is outside the scope of this paper. Although the characteristics of the SOL also influence the RF-induced sputtering process (as e.g. the light impurity content and its energy), one effect that most likely plays a strong role is that by locally increasing the electron density close to the ICRF antennas, the excited RF fields are reduced leading to weaker RF rectified field acceleration of the SOL ions. Simulations performed with a 2D RF wave code that uses a simplified version of the antenna geometry but includes poloidal field effects and adopts a full cold plasma dielectric tensor that describes the excitation of both fast and slow waves [4] indicate a significant reduction of the RF fields when the density in front of the antennas is increased from zero to $\sim 2 \times 10^{18}/m^3$. In these conditions, the parallel component of the RF electric field - believed to be the main responsible for RF sheath effects – is strongly suppressed, both due to the lower excitation voltages (higher coupling) needed per MW of launched power and in particular due to the increased parallel electron mobility at higher densities. The decrease of the poloidal component with density is less pronounced since it is mainly related to the gradual reduction of the fast wave evanescence layer at larger SOL densities leading to improved antenna-plasma coupling and therefore lower strap voltages for given input power.

Finally, the somewhat larger ELM frequencies observed with main chamber gas injection (in particular with top-injection) can also contribute to the lower levels of impurities measured when switching from divertor to main chamber fuelling, as described in [23].

5. Summary

Recent JET-ILW experiments have shown that the far-SOL density profiles can be tailored to optimize the coupling of ICRF waves in high power H-mode discharges using main chamber deuterium

fuelling. The strongest effect was observed with outer mid-plane injection on antennas located at the proximity of the gas injection inlet and coupling resistance improvements of up to $\Delta R/R \sim 100\%$ with respect to divertor fuelling were observed. Dedicated studies have shown that in this case the coupling enhancement can be strongly localized – with a toroidal decay length of $\sim$2 m (0.5 rad) around the injection point – and is mainly associated to the diffusion of neutrals in the vicinity of the ICRF antennas, including the poloidal limiter shadow region. Top gas injection has a weaker ($\Delta R/R \sim 50\%$) but global – toroidally symmetric – influence on the coupling of all the ICRF antennas, suggesting that enhanced ionization of the injected neutral cloud in flux tubes magnetically connected to the antennas is the main player on the far-SOL density tailoring in this case. By using a gas mixture of mid-plane and top injection valves, the coupling resistances of the four toroidally distributed ICRF antennas were simultaneously optimized and in these conditions $\sim$6 MW of ICRF power was routinely coupled to ELMy H-mode discharges with $P_{nbi} > 15$ MW.

Although switching the gas fuelling location did not have a strong impact in the plasma core and pedestal properties nor on the plasma confinement, the SOL properties as e.g. the neutral particles distribution as well as the impurity levels were modified. In particular, the W and Ni concentrations, induced by sputtering of energetic ions accelerated by RF sheath rectification effects during high power ICRH, are lower when using main chamber fuelling than with divertor fuelling. This could be related to the reduction of the poloidal and toroidal RF field amplitudes generated in the SOL close to the ICRF antennas due to the local increase of the far-SOL density profiles, but deeper studies are necessary to identify the actual mechanism causing the mitigation of RF sheaths with localized gas injection.

The here reported studies support the idea that in ITER, where the antenna-plasma distances are larger (lower RF coupling) than in current-day machines, the optimization of gas injection using main chamber fuelling can have a significant impact on the overall performance of the ICRF system.

Acknowledgements

This work was supported by EURATOM and carried out within the framework of the European Fusion Development Agreement. The views and opinions expressed herein do not necessarily reflect those of the European Commission.

References

[1] G. Matthews et al., Phys. Scr. 2011 (2011) 014001.
[2] S. Brezinsek, et al., this issue.
[3] L. Colas, et al., this issue.
[4] D. Van Eester et al., Plasma Phys. Control. Fusion 55 (2013) 025002.
[5] P. Jacquet et al., Nucl. Fusion 51 (2011) 103018.
[6] V. Bobkov et al., AIP Conf. Proc. 1187 (2009) 125.
[7] A. Czarnecka et al., Plasma Phys. Control. Fusion 54 (2012) 074013.
[8] D. Van Eester et al., Plasma Phys. Control. Fusion 55 (2013) 055001.
[9] R. Neu et al., Plasma Phys. Control. Fusion 49 (12B) (2007) B59–B70.
[10] M. Goniche et al., Paper O4.129, EPS Conference, Berlin, 2014.
[11] M. Valisa et al., Nucl. Fusion 51 (2011) 033002.
[12] C. Angioni et al., Phys. Plasmas 14 (2007) 055905.
[13] M. Graham et al., Plasma Phys. Control. Fusion 54 (2012) 074011.
[14] E. Lerche, et al., IAEA FEC 2014, St. Petersburg, Russian Federation.
[15] V. Bobkov et al., AIP Conf. Proc. 1580 (2014) 271.
[16] P. Jacquet et al., Nucl. Fusion 52 (2012) 042002.
[17] M.-L. Mayoral et al., AIP Conf. Proc. 933 (2007) 55.
[18] P. Jacquet, et al., IAEA FEC 2014, St. Petersburg, Russian Federation.
[19] A. Sirinelli et al., Rev. Sci. Instrum. 81 (10) (2010) 10D939.
[20] V. Bobkov et al., J. Nucl. Mater. 438 (2013) S160–S165.
[21] T. Pütterich et al., Plasma Phys. Control. Fusion 50 (2008) 085016.
[22] A. Czarnecka et al., Plasma Phys. Control. Fusion 53 (2011) 035009.
[23] N. Fedorzak, et al., this issue.